Temperature and Electrolyte Optimization of the α-Hemolysin Latch Sensing Zone for Detection of Base Modification in Double-Stranded DNA

Robert P. Johnson, Aaron M. Fleming, Qian Jin, Cynthia. J. Burrows and Henry. S. White*

white@chem.utah.edu

Department of Chemistry, University of Utah, 315 S. 1400 East, Salt Lake City, Utah, 84112-0850.

Abstract

The latch region of the wild-type protein pore α-hemolysin (α-HL) constitutes a sensing zone for individual abasic sites (and furan analogues) in double-stranded DNA (dsDNA). The presence of an abasic site or furan within a DNA duplex, electrophoretically captured in the α-HL vestibule and positioned at the latch region, can be detected based on the current blockage prior to duplex unzipping. Variations in blockage current were investigated as a function of temperature (12 – 35 °C) and KCl concentration (0.15 – 1.0 M) to understand the origin of the current signature and to optimize conditions for identifying the base modification. In 1 M KCl solution, substitution of a furan for a cytosine base in the latch region results in an ~8 kJ mol^{-1} decrease in the activation energy for ion transport through the protein pore. This corresponds to a readily measured ~2 pA increase in current at room temperature. Optimal resolution for detecting the presence of a furan in the latch region is achieved at lower KCl concentrations, where the noise in the measured blockage current is significantly lower. The noise associated with the blockage current also depends on the stability of the duplex (as measured from the melting temperature), where a greater noise in the measured blockage current is observed for less stable duplexes.

Introduction

The wild-type pore-forming toxin α-hemolysin (α-HL) has been studied extensively over the past decade as a platform for ion-channel recordings of single-stranded DNA (ssDNA) (1-7). By applying a potential difference across an α-HL pore that is embedded into a lipid membrane, DNA can be driven electrophoretically from one side of the pore to the other. The current is recorded as a function of time, and translocations of the individual DNA strands are observed as 'events' in which the current momentarily decreases (8, 9). The extent of this current change is dependent on the sequence of the DNA near the tightest constriction of the protein channel, which is comparable to the diameter of ssDNA.

While ssDNA can translocate through α-HL, double-stranded DNA (dsDNA) does not because its diameter (~ 2.0 nm) is larger than the narrowest constriction of the pore, ~1.4 nm (10). However, it is possible to capture dsDNA in the α-HL vestibule, and this technique has been used to interrogate dsDNA hairpins within the vestibule of α-HL to reveal structural composition (11, 12) to study escape kinetics (13), and to probe the electrical potential distribution within the α-HL protein pore (14). With an appropriate applied voltage (120 mV), dsDNA will 'unzip' (denature) into its constituent components (11, 15-19) (Fig 1A). In a typical experiment, dsDNA with an additional single-stranded poly-T tail is driven into α-HL from the *cis* (vestibule) side of the channel. The duplex is driven down to the 1.4 nm constriction (15) that separates the vestibule from the β-barrel, through which the duplex cannot pass. The electrophoretic driving force causes the double-stranded section to unzip into its constituent components.

The time taken for the unzipping to occur, which is on the order of milliseconds, is dependent on the length and composition of the DNA (19, 20) and correlates with the

stability of the duplex (15, 19, 20). This feature has been used previously to identify the presence of damage sites in DNA that destabilize the duplex (15, 21).

The decrease in current while dsDNA is captured in the pore, relative to the current measured through an open channel, is a result of the blocking contributions from both the single-stranded and double-stranded sections of DNA. While the majority of the current is blocked by the poly-T tail that resides in the -barrel during unzipping, there is also a contribution to the current blockage by the double-stranded section that resides in the vestibule. In our previous work, we have shown that removing a single base in the duplex section (by replacing it with a furan group or abasic site) can result in an increase in measured current through the pore. The precise change in current is dependent on the position of the missing base in the sequence relative to the latch constriction of the -HL protein pore (Fig 1C).

In this article, we demonstrate that the difference in observed current can be attributed to the differences in activation energy for transport of the electrolyte (K^+ and Cl^-) through the latch region of $\alpha-HL$ during dsDNA residence inside the pore. Through temperature- and KCl-dependent measurements, we show how identifying a furan group at the latch can be optimized at lower temperatures and lower KCl concentration. In particular, the noise associated with the current measured during unzipping increases with increasing KCl concentration. Finally, we demonstrate for the first time that the noise associated with the current measured during unzipping is dependent on the stability (as measured from the melting temperature) of the DNA duplex. This finding we ascribe to "breathing" of the duplex within the vestibule. While previous efforts at nanopore measurements of DNA have focused on translocation of ssDNA, (1-7) the effective exploitation of the latch sensing zone offers exciting

possibilities for characterizing and sequencing the more biologically relevant dsDNA along with its modifications.
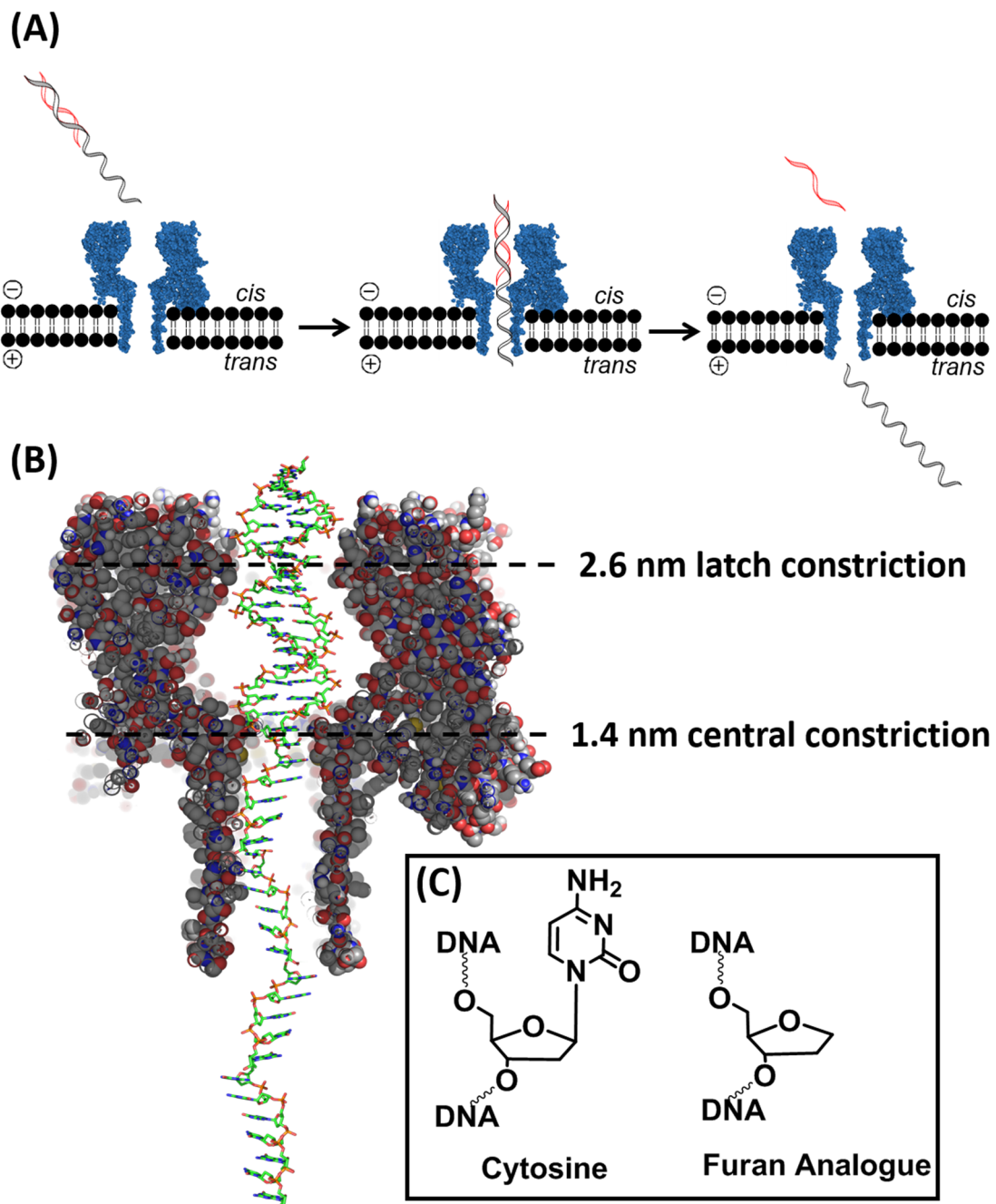
(A)

(B)

2.6 nm latch constriction

1.4 nm central constriction

(C) Cytosine

Furan Analogue

Fig. 1. (A) The unzipping of dsDNA in the ⍺-HL nanopore. DNA denatures or 'unzips' into its constituent components when a voltage of 120 mV is applied across the pore. (B) Upon capture, the duplex section is driven down to the central 1.4 nm constriction and pauses momentarily before unzipping. (C) Replacing a cytosine base by a furan

group in proximity to the latch constriction results in an increase in measured current prior to unzipping. The α-HL structure was taken from pdb 7AHL, and the DNA structure is shown on a 1:1 scale with α-HL (10).

Results & Discussion

The DNA sequence chosen for study was a portion of the *KRAS* gene, 5'-(T)$_{24}$-TGGAGCTGCTGGCGTAG, with the poly-T tail added to assist in threading through the nanopore. This sequence is of interest because damage that gives rise to point mutations within this gene can lead to uncontrolled cell growth and human carcinoma. (22) The 41-mer sequence of interest was hybridized to a complementary 17-mer to form a 17-base pair duplex section. The capture and unzipping of these DNA duplexes within α-HL was continuously monitored, and the measured current of each event was used to construct histograms of the blocking current and noise.

When a single base was removed from the DNA sequence at the latch region and replaced with a furan (Fig. 1C), the measured current through the pore increases relative to the fully complementary sequence (Fig. 2). The measured current difference between the complementary duplex and the duplex containing a furan at the latch region was ~2 pA.
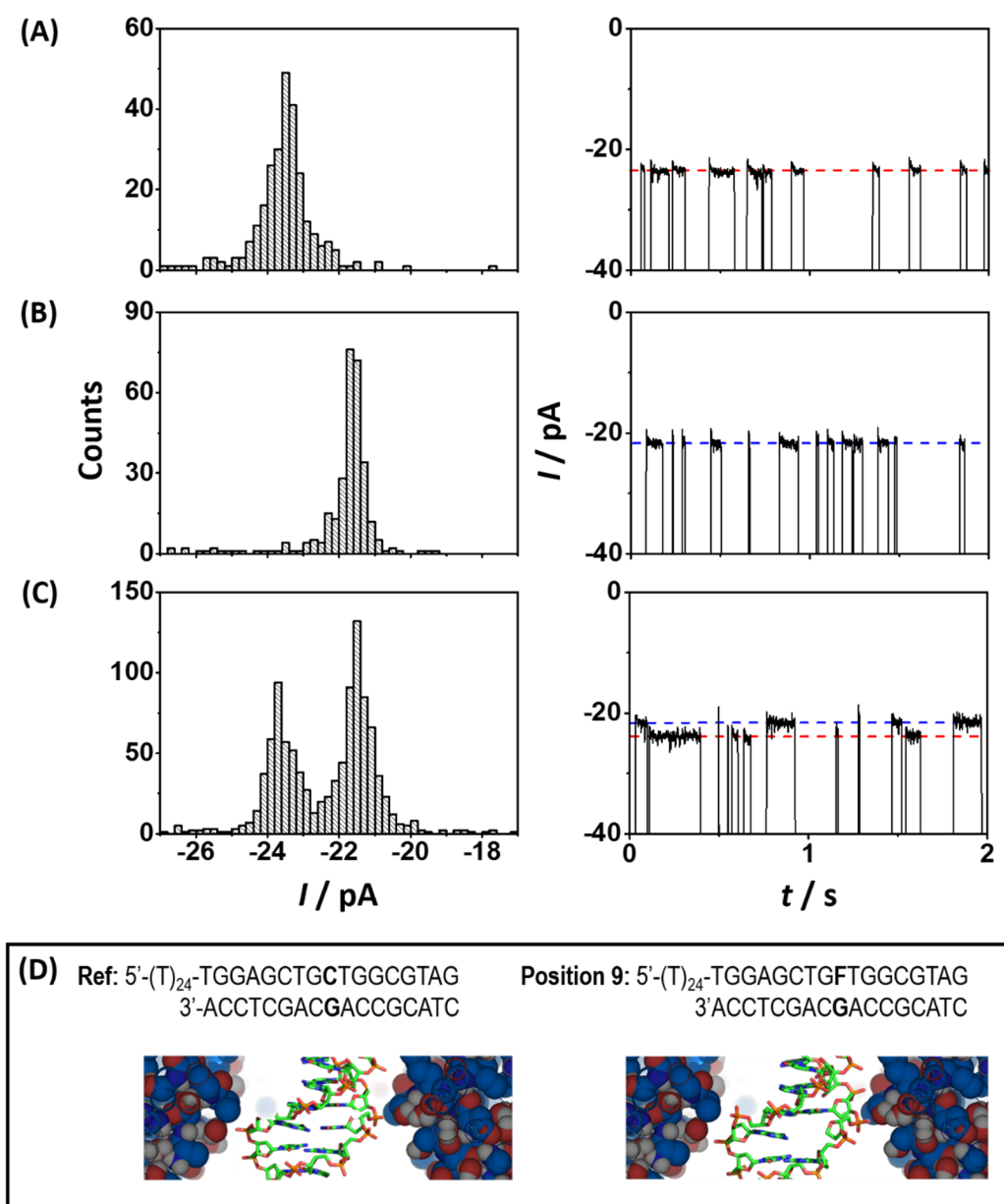
Fig 2. Resolving the presence of a single furan , an abasic mimic, in a DNA duplex. Current histograms and representative current time traces illustrating the observed unzipping event currents for (A, red line) duplex containing a furan group at position 9F, (B, blue line), the reference duplex (containing no modifications), and (C) both the furan-containing and reference duplex. (D) The approximate position of the furan group, relative to the latch region in -HL is shown for the reference and furan-containing duplexes.

Defining the Extent of the Latch Sensing Zone

In an earlier publication, we demonstrated that moving the position of the furan altered the observed current relative to the reference (21). These preliminary experiments were performed in a buffer containing 150 mM KCl, chosen because the initial studies focused on monitoring the uracil-DNA glycosylase (UDG) catalyzed conversion of a uracil base to an abasic site, and the UDG enzyme is catalytically inactive at higher KCl concentrations. (19) Such a low KCl concentration is unusual in nanopore measurements employing -HL, because there the rate of capture of DNA is significantly reduced by repulsive electrostatic interactions between negative amino acid residues at the vestibule opening and the phosphate backbone of DNA (9, 23). These interactions are much more effectively screened at higher KCl concentrations.

We studied the difference in blocking current, I, as a function of sequence position, between a DNA duplex modified with a single-furan site and an unmodified dsDNA reference containing standard Watson-Crick base pairs (Fig. 3) The position of the furan modification in the DNA was varied between 6 and 13 base pairs from the 3' end of the 17-mer (i.e. 6 to 13 base pairs *cis* to the central constriction). The position of the furan site within the latch region of -HL before unzipping determines the blocking current, defining a sensing zone that spans approximately 6 base-pairs (~2 nm). At the center of this sensing zone, the differences in blocking currents between the furan-containing and reference duplex reaches a maximum of just over 2 pA, corresponding to a readily detectable 1.6% change when the unzipping event current is normalized relative to the open channel current (I/I_o). On either side of this maximum, the current difference tends toward zero over 2- 3 base pairs.

I values recorded in 1 M KCl (Fig. 3) are similar to values previously measured in 0.15 M KCl (21). This is an important finding because it demonstrates the general

applicability of the latch sensing zone to interrogate DNA structure at electrolyte concentrations commonly used for ion channel recordings.

Assuming the distance between base pairs remains ~0.34 nm in the vestibule under an electric force, (24) this range of base pairs corresponds to a distance of between 2.0 and 4.4 nm, placing the furan group at a narrowing of the protein vestibule during unzipping, as shown in Fig 1B. This latch site, as first described in detail by Song et al., is approximately 2.6 nm in diameter (10), comparable to the diameter of dsDNA (2.0 nm).

Structural changes in DNA hairpins have previously been identified using the vestibule of -HL by Vercoutere and co-workers (11). In one experiment, they observed a 2 pA decrease in measured current when a dsDNA hairpin is altered only by adding an additional T to the loop section. This loop section is situated at distance equivalent to 6-7 base pairs from the central constriction of -HL, placing it at the edge of the latch constriction during vestibule residence. Their observation is in agreement with our results, where placing the additional T in the latch region of -HL contributes to the decrease in measured current, much like the presence of a missing base (furan group) in our experiments results in a current increase.
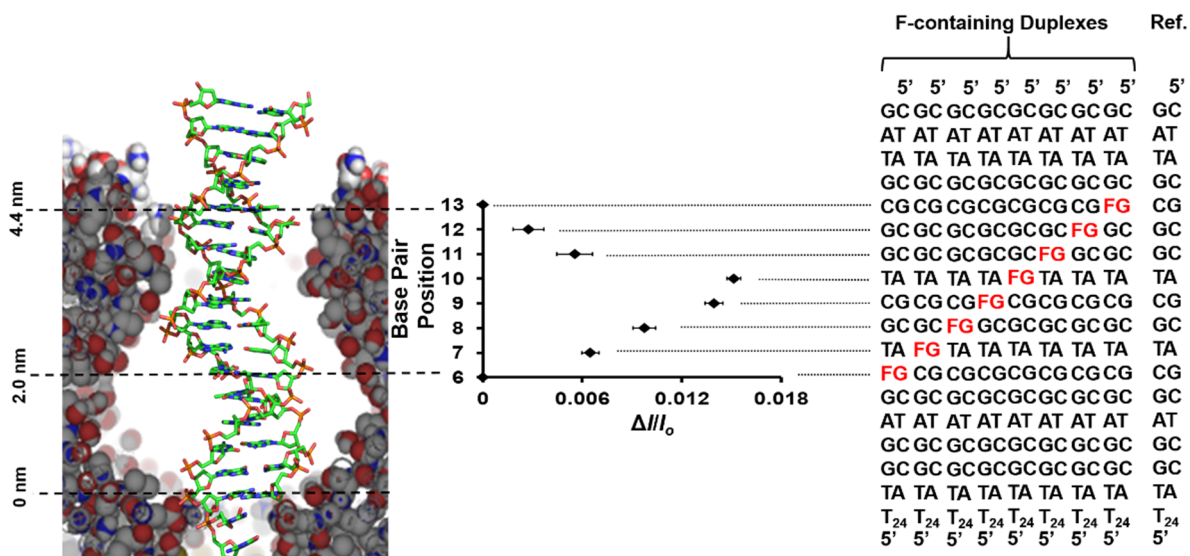
Fig. 3. Mapping the resolution of the latch sensing zone within α-HL in a 1 M KCl solution. The current was monitored for a series of duplexes in which the position of the furan group was moved systematically through the sequence while maintaining a guanine opposite the furan. The differences in the blocking current ΔI for the furan-containing duplex relative to the (fully complementary) reference duplex, normalized to the open channel current, I_0, are plotted vs. the position of the furan. The approximate position of the furan substitution relative to the α-HL vestibule is shown. Error bars are given as the standard error of the mean. The α-HL structure was taken from pdb 7AHL (10), and the DNA structure is shown on a 1:1 scale with α-HL.

Effect of Temperature

Temperature-dependent measurements were performed in order to better understand the origin of the increase in current when a furan was placed into the proximity of the latch region. As the temperature was increased from 12 to 35 °C, the currents of both the open channel and the unzipping events increased, in accordance with the expected increase in ion mobilities (23). Over this temperature range, the tertiary structure of the protein is believed to be stable (25). However, the current difference between the duplex containing a furan at the latch (position 9F) and a duplex with a furan situated outside the latch (position 13F) becomes smaller with increasing temperature as shown in Fig. 4.
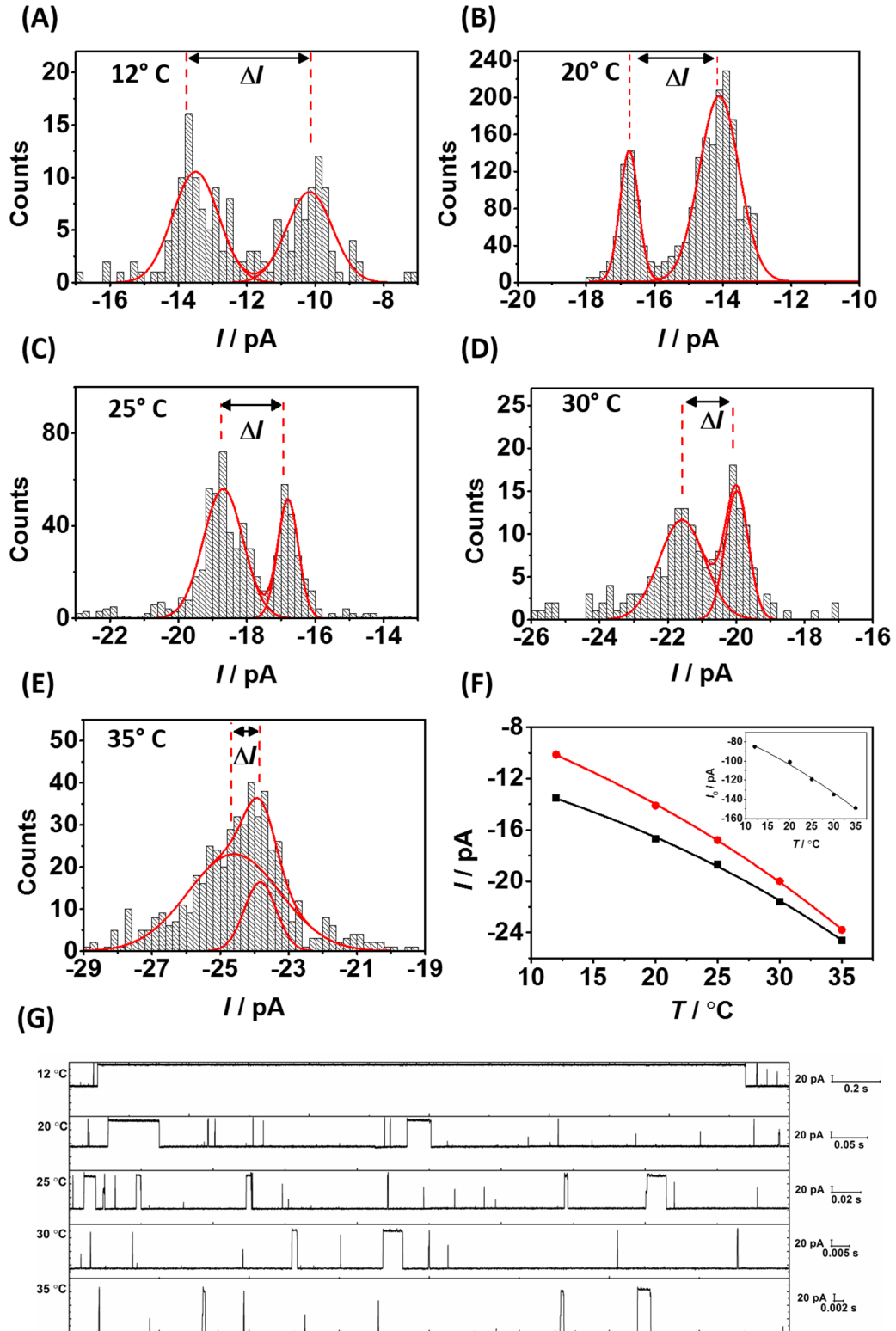
Fig. 4. The effect of temperature on the observed current during unzipping of two duplexes, one of which has a furan group situated at the latch region of -HL during unzipping (position 9F), and one that does not (position 13F). (A-E) Representative

temperature-dependent current histograms illustrating the change in the current (and current difference) measured during unzipping. (F) The change in the current during unzipping as a function of temperature for position 9F (black squares) and position 13F (red circles); and change in current for the open channel (inset). (G) *I-t* traces as a function of temperature. Events < 2 ms in duration are attributed to excess DNA and/or collision of the DNA with the protein surface.

The origin of the dependence of the current on the position of the furan was explored by measuring the activation energy for electrolyte transport through the nanopore. The activation energy reflects the resistance to electrolyte transport when dsDNA is introduced into the vestibule, and was determined by measuring *I* as a function of temperature and analysing the data using the linearized version of the Arrhenius equation:

$$\ln(I) = -\frac{E_A}{RT} + \ln(C) \qquad (1)$$

where *R* is the gas constant, *T* is the temperature and *C* is the pre-exponential factor.

Arrhenius plots for the open channel, and the two duplexes with the furan group situated inside and outside of the latch region (positions 9F and 13F, respectively), were constructed from the data in Fig. 4 and are shown in Fig. 5. The calculated activation energy for the open channel measured at an applied potential of 120 mV was 17.1 ± 0.6 kJ mol^{-1}. This is comparable to the activation energy for diffusion of KCl in bulk solution (17.7 kJ mol^{-1}) (26).

A significant increase in the activation energy for electrolyte transport (relative to the open channel) was observed when dsDNA was situated inside the pore (i.e., during unzipping). This reflects a decrease in the mobility of ions within the pore,

caused by the presence of DNA that occupies a significant volume of the vestibule, and/or specific interactions of the ions with the DNA duplex. The activation energy was also highly dependent on the position of the missing base within the sequence. When the furan group was situated inside the latch region of -HL, the activation energy at (120 mV) was significantly lower (19 ± 1 kJ mol^{-1}) than when it was situated outside the latch region (27 ± 1 kJ mol^{-1}). The activation energy under the same conditions for the perfectly-complementary reference duplex (containing no furan sites) was found to be identical (29 ± 2 kJ mol^{-1}) to the duplex with the furan positioned outside the latch region (Fig SI-6). We speculate that the decrease in activation energy reflects less steric hindrance at the constriction site, where removal of a base opens a passage through which the ions can move more freely. Our data predicts that at higher temperatures (>35 °C) the difference in the measured currents for the two duplexes is inverted. That is, a duplex with a furan at position 9F would become more blocking than a duplex with a furan position 13F. While this effect is interesting, measurements beyond 35 °C are challenging because the decreasing residence time of the DNA at higher temperatures, due to the exponential increase in the unzipping rate, results in a much poorer signal to noise ratio and prohibits reliable determination of the blockage currents.
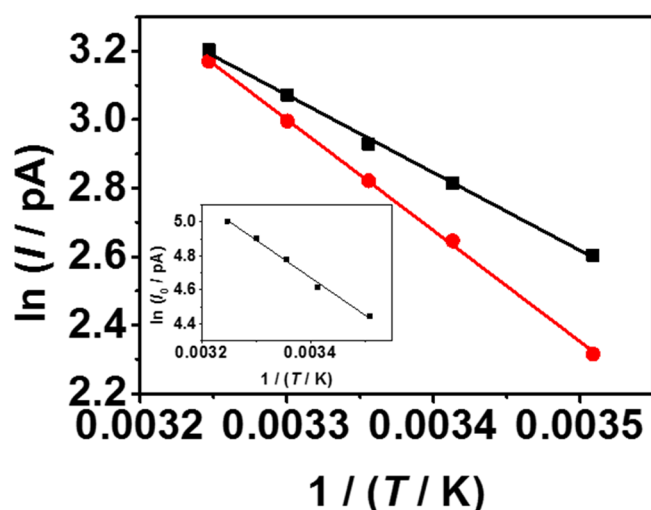
Fig. 5. Determining the activation energy of electrolyte transport from an Arrhenius plot. The change in current as a function of the reciprocal temperature during unzipping of DNA duplex containing a furan at position 9F (black squares), position 13F (red circles), and for the open channel current (inset). Details of the sequences studied are given in Fig. 3.

It is also clear that measurements at lower temperatures have a distinct advantage in resolving the presence of a missing base in the latch region. This is because the current difference between a furan-containing duplex and the reference was greatest (Fig. 4F) and the noise is lower (4G). However, this advantage is balanced against the increased length of the unzipping event time, which increases exponentially as the temperature decreases (Fig 4G & SI-7).

Effect of KCl Concentration

A series of unzipping experiments using duplexes containing a furan positioned in the latch (position 9F) and distal to the latch (position 13F) of -HL, as shown in Fig. 3, were conducted over a range of KCl concentrations between 0.15 and 1 M to further optimize detection of abasic/furan sites. The objective of these experiments was to identify how the difference in blocking current between two duplexes varies as a function of KCl concentration.

It is known that the current of an open -HL channel increases as a function of electrolyte concentration (21). While the effect of KCl concentration on ssDNA translocation has been studied previously (23), the dependence of blockage current prior to dsDNA unzipping on electrolyte concentration has not been reported.

The measured current during unzipping for both duplexes increases with an increase in KCl concentration up to about ~0.3 M, at which point the current remains fairly constant (Fig. 6). Below 0.15 M (outside the measurable range) the current is expected to decrease towards a limiting value determined by the counterions associated with the fixed charges on the wall of the protein and/or DNA duplex. The levelling-off in the observed current occurs at a similar concentration to that previously observed for ssDNA translocation (23). In this concentration region, the number of current-carrying ions inside the pore during DNA unzipping is only weakly dependent on the external KCl concentration between 0.3 and 1 M. We speculate that this due to exclusion of anions from the pore by the negative charge of the sugar-phosphate backbone. This is in contrast to the behavior of the open channel current, which increased linearly with increasing KCl concentration over the range studied (inset of Fig. 6).

Further evidence for a constant number of ions in the -HL channel above 0.3 M KCl may be inferred from analyzing the time taken to unzip the DNA duplex inside the -HL channel. We find also remains constant as a function of KCl concentration between 0.3 and 1 M (Fig. SI-5). If the KCl concentration inside the protein pore increased with increasing bulk KCl concentration, and assuming that the stability of DNA as a function of KCl concentration in the confined geometry of -HL is similar to that in bulk solution, then an increase in unzipping times with increasing KCl concentration is to be expected. This is because the unzipping time is related to the stability of the DNA duplex, and the latter increases as a function of KCl concentration due to more effective screening of adjacent negatively charged phosphate groups (27).
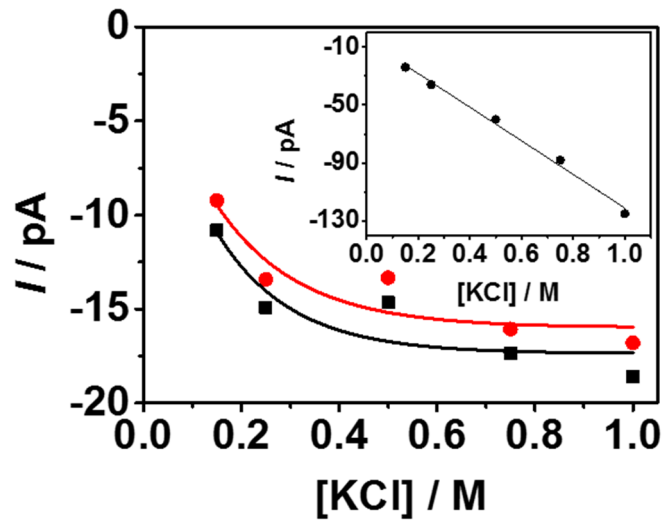
Fig. 6. The effect of KCl concentration on the blocked channel current during dsDNA unzipping. Inset: the open channel current increases linearly as a function of KCl concentration. Currents were recorded at 120 mV in a 10 mM phosphate (pH 7.5) solution containing 0.15 – 1 M KCl. Current histograms for each KCl concentration are shown in Fig. SI-3.

Effect of Electrolyte Concentration on Current Noise

A single blockage current event has an associated noise. For example, if a blockage current is reported as -21.6 ± 0.8 pA, then the noise associated with that one event is 0.8 pA. The noise from many events can be used to construct a histogram of blocking current noise (Figs. 7A and 7B). In general, we find that the noise distribution for unzipping events is skewed-right toward higher noise. The average noise associated with the unzipping of a duplex can be estimated from the median of this distribution.

The noise associated with the unzipping was examined as a function of KCl concentration (Fig. SI-8) for the two duplexes with a furan situated outside of the latch region during unzipping (position 13F) and inside the latch region (position 9F). The noise associated with open channel events (i.e., the events between DNA capture) was also measured (Fig. 7; inset). The event rate for ssDNA is greatest at high KCl concentrations (23). However, this is not necessarily the optimum electrolyte concentration in which unzipping experiments should be performed. This is because the median of the noise was found to increase with the increasing KCl concentration. (Fig. 7).

At 150 mM KCl, the median of the blockage event noise (for DNA with a furan at position 13F) is 1.23 ± 0.07 pA. This increases to 1.9 ± 0.1 pA at 1 M KCl. The open channel current event noise in this particular experiment increases to 2.25 ± 0.09 pA. While the results presented earlier show that the latch region is capable of resolving the presence of a furan at 1 M KCl, it is clear that optimal resolution is obtained in KCl concentrations at or lower than 0.5 M, where the noise in the measured current is lower. Clearly, both KCl concentration and temperature are important to consider when choosing the measurement conditions for identifying abasic sites in DNA. Optimal conditions are therefore anticipated at low electrolyte concentration and low

temperature, where current-peak separation is at a maximum and the noise in the current is at a minimum. At high electrolyte concentration and high temperatures, resolving the presence of a furan would be extremely challenging.
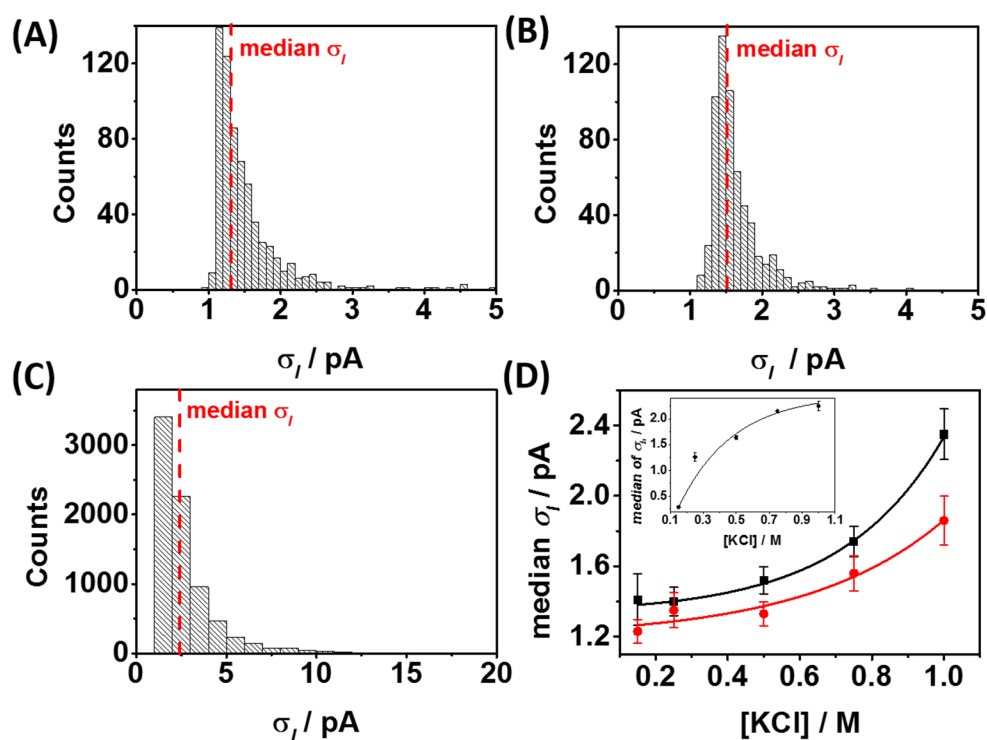

Fig. 7. Representative histograms of the noise in the measured unzipping currents for a duplex with a furan at (A) position 9F and (B) position 13F in 0.75 M KCl. (C) The open-channel noise distribution (the noise of the current measured between unzipping events). The dashed red lines denote the median of the noise distribution. (D) The effect of KCl concentration on the median of the noise for a furan at position 9F (black lines), position 13F (red lines) and the open channel current events (inset). Histograms of the event noise at each KCl concentration are shown in Fig SI-8.

The noise in the measured current during unzipping also appears to be dependent on the stability of the duplex. In Fig. 7D, the duplex with the furan at position 9F (black line) exhibits a consistently higher noise than the duplex with the furan at position 13F (red line) between 0.15 and 1 M KCl. The melting points of these two duplexes are 60.7

± 0.6 °C and 64.6 ± 0.6 °C, respectively, suggesting that the noise level in the unzipping event current is higher for less stable duplexes.

To verify this observation, the melting temperatures of all the duplexes used in the mapping studies presented earlier were measured, and the noise of the unzipping events for each were analyzed (Fig. SI-9). Fig. 8 shows the change in the median of the unzipping event noise normalized with the respect to the median of the open channel event noise, as a function of duplex stability.
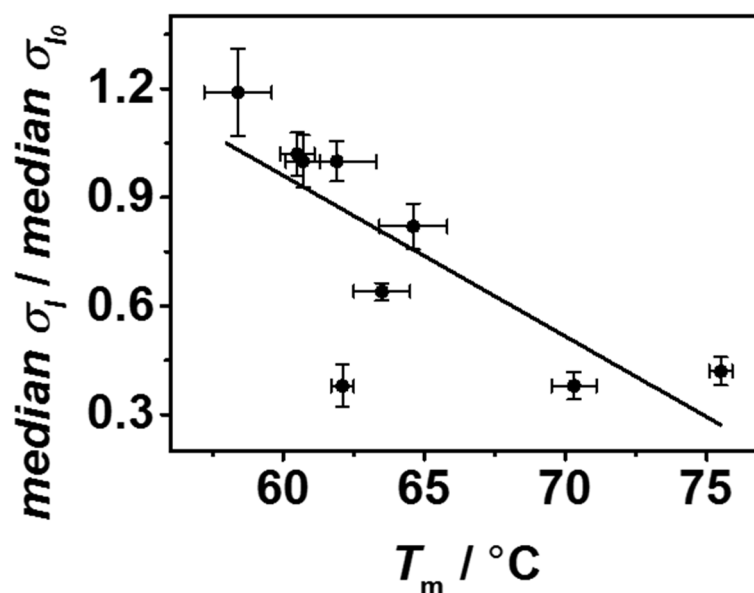

Fig. 8. The effect of melting temperature on the noise of the unzipping event currents. The median of the noise associated with each unzipping event current, normalized to the noise of the open channel current increases as the stability of the duplex decreases. A constant temperature of 25 °C was used for all nanopore measurements. Error bars on the *y*-axis are the standard error of the median, and error bars on the *x*-axis are twice the standard deviation of three averaged melting point experiments. Histograms of the noise of the unzipping events for each duplex studied are given in Fig. SI-9.

An increase in the noise of the unzipping events is observed as the duplexes become less stable. DNA is a dynamic structure, and it is reasonable to assume that during occupation of the -HL channel, the DNA undergoes local conformational changes. Such conformational changes are important in the concept of DNA "breathing" that leads to the breaking of localised base-pairs and the formation of ssDNA regions (DNA "bubbles") that have a lifetime of ~ 100 µs (28-30). For less stable duplexes (as measured by the melting temperature) these conformational changes are likely to be larger and more frequent when the DNA is situated inside the -HL channel prior to unzipping. We speculate that these fluctuations in local conformation contributed to the measured current noise.

Conclusions

We have demonstrated that the latch region of -HL constitutes a sensing zone that is capable of detecting a furan group in dsDNA over a range of 4-5 base pairs. The presence of a furan group in the latch region during unzipping gave rise to an increase in current relative to the unzipping of duplex that has a fully-complementary sequence.

The results presented here demonstrate that the detection of mutation-causing abasic sites in the *KRAS* sequence using nanopore unzipping can be optimized by using low electrolyte concentration (150 mM) and low temperature (12 °C) conditions where the noise associated with individual events is at a minimum and the current signature resolution between an abasic site-containing duplex and the reference is at a maximum. One potential route to further optimization is through reducing the DNA breathing effect that leads to the noise in individual events. One potential route to decreasing DNA breathing is through the use of a DNA probe constructed from an analogue such as peptide nucleic acid (PNA), which forms a more stable structure (31). Clearly, the latch

constriction of -HL, which is specific to dsDNA, offers the potential to study and detect site-specific changes in duplex structure of biological relevance, such as mutations and damage to individual bases.

Experimental Section

DNA Preparation and Purification Procedures

DNA was prepared from commercially available phosphoramidites (Glen Research, Sterling, VA) by the DNA Core Facility at the University of Utah. Afterwards, DNA oligomers were cleaved from the solid support and deprotected following the manufacturer's protocol, followed by purification using an ion-exchange HPLC column running a linear gradient of B from 25% to 100% over 30 min while monitoring UV absorbance at 260 nm (A = 20 mM NaP_i, 1 M NaCl, pH 7 in 10% CH_3CN/90% ddH_2O, B = 10% CH_3CN/90% ddH_2O, flow rate = 3 mL/min).

Chemicals and Materials for Nanopore Measurements

All buffer solutions used were prepared as 10 mM phosphate (pH 7.5), with a KCl concentration as indicated. WT -HL was purchased from List Biological Laboratories in the monomer form of lyophilized powder and dissolved in water at 1 mg/mL. 1,2-Diphytanoyl-*sn*-glycero-3-phospho-choline (DPhPC) was dissolved in decane at 10 mg/mL and used to form the bilayer. The bilayer was supported by a glass nanopore membrane (GNM), the fabrication of which has been described previously (32). Glass nanopore membranes were modified with a 2% (v/v) (3-cyanopropyl) dimethylchlorosilane in acetonitrile to create a moderately hydrophobic surface. The DNA duplexes were annealed by mixing the 41-mer and 17-mer at a 1:2 mole ratio, followed by heating in a 90 °C water bath for 5 min and then cooling to room temperature over 3 h.

Current-Time Recordings

Current-time (*i-t*) recordings were performed using the low noise Nanopatch system (Electronic BioSciences, Inc., San Diego, CA), which is also capable of temperature control to an accuracy of ± 0.5 ° C. Temperature control is achieved by a thermo-electric peltier embedded underneath the solution reservoir (outside the capillary), and measured by a K-Type thermocouple in contact with the solution. The temperature was permitted to equilibrate for 5 minutes before measurement. The KCl solution was used as the electrolyte to fill the solution reservoir and the GNM capillary. A voltage was applied across the GNM between two Ag/AgCl electrodes placed inside and outside of the capillary. As previously described, a lipid bilayer was deposited across the GNM orifice as indicated by a resistance increase from ~10 M (associated with the open GNM) to ~100 G . (32) A pressure of 60 to 80 mmHg was applied to the inside of the GNM capillary using a syringe, allowing the lipid bilayer to be functional for the protein channel reconstitution (32). Next, 0.2 µL of -HL monomer solution at 1 mg/mL was added to the *cis* side of GNM (a volume of 350 µL). The duplex DNA (15 µM) was added to the solution reservoir after protein reconstitution into the lipid bilayer, which was indicated by a single jump in current by approximately 1 pA /mV at 25 ° C. A voltage of 120 mV was applied *trans vs. cis*, (Ag/AgCl electrode inside the capillary *vs* Ag/AgCl electrode placed at external solution (cis negative).). The *i-t* traces were filtered at 10 kHz and sampled at 50 kHz.

Data Collection

Based on previous reports, (19) *I-t* blockades that lasted longer than 2 ms were identified as DNA unzipping events. Shorter events were attributed to translocation of excess single-stranded DNA (ssDNA), and/or collision of the DNA with the protein

surface. The current amplitude of each blockade was used to determine the identity of duplex, as described in the main text. Events were extracted using QuB (version 1.5.0.31). Histograms of current, noise and unzipping durations were generated and plotted using Origin Pro (version 9.0). Details of error treatment are given in the supplementary information.

Supporting Information

Full DNA sequence details, representative current-time transients, additional current and current-noise histograms, additional activation energy data, unzipping-time analysis and error calculations.

Acknowledgments

References

1.	Akeson, M., D. Branton, J. J. Kasianowicz, E. Brandin, and D. W. Deamer. 1999. Microsecond time-scale discrimination among polycytidylic acid, polyadenylic acid, and polyuridylic acid as homopolymers or as segments within single RNA molecules. Biophys. J. 77:3227-3233.
2.	Kasianowicz, J. J., E. Brandin, D. Branton, and D. W. Deamer. 1996. Characterization of individual polynucleotide molecules using a membrane channel. Proc. Natl. Acad. Sci. USA 93:13770-13773.
3.	Meller, A., L. Nivon, E. Brandin, J. Golovchenko, and D. Branton. 2000. Rapid nanopore discrimination between single polynucleotide molecules. Proc. Natl. Acad. Sci. USA 97:1079-1084.
4.	Purnell, R. F., and J. J. Schmidt. 2009. Discrimination of single base substitutions in a DNA strand immobilized in a biological nanopore. ACS Nano 3:2533-2538.
5.	Reiner, J. E., A. Balijepalli, J. W. F. Robertson, J. Campbell, J. Suehle, and J. J. Kasianowicz. 2012. Disease detection and management via single nanopore-based sensors. Chem. Rev. 112:6431-6451.
6.	Stoddart, D., A. J. Heron, J. Klingelhoefer, E. Mikhailova, G. Maglia, and H. Bayley. 2010. Nucleobase recognition in ssDNA at the central constriction of the -hemolysin pore. Nano Lett. 10:3633-3637.
7.	Stoddart, D., G. Maglia, E. Mikhailova, A. J. Heron, and H. Bayley. 2010. Multiple base-recognition sites in a biological nanopore: two heads are better than one. Angew. Chemie 122:566-569.
8.	Kasianowicz, J. J., J. W. F. Robertson, E. R. Chan, J. E. Reiner, and V. M. Stanford. 2008. Nanoscopic porous sensors. Ann. Rev. Anal. Chem. 1:737-766.
9.	Wanunu, M. 2012. Nanopores: a journey towards DNA sequencing. Phys. Life Rev. 9:125-158.
10.	Song, L., M. R. Hobaugh, C. Shustak, S. Cheley, H. Bayley, and J. E. Gouaux. 1996. Structure of staphylococcal alpha-hemolysin, a heptameric transmembrane pore. Science 274:1859-1866.
11.	Vercoutere, W., S. Winters-Hilt, H. Olsen, D. Deamer, D. Haussler, and M. Akeson. 2001. Rapid discrimination among individual DNA hairpin molecules at single-nucleotide resolution using an ion channel. Nat. Biotech. 19:248-252.
12.	Vercoutere, W. A., S. Winters-Hilt, V. S. DeGuzman, D. Deamer, S. E. Ridino, J. T. Rodgers, H. E. Olsen, A. Marziali, and M. Akeson. 2003. Discrimination among individual Watson–Crick base pairs at the termini of single DNA hairpin molecules. Nuc. Acids Res. 31:1311-1318.
13.	Lathrop, D. K., E. N. Ervin, G. A. Barrall, M. G. Keehan, R. Kawano, M. A. Krupka, H. S. White, and A. H. Hibbs. 2010. Monitoring the escape of DNA from a nanopore using an alternating current signal. J. Am. Chem. Soc. 132:1878-1885.
14.	Howorka, S., and H. Bayley. 2002. Probing distance and electrical potential within a protein pore with tethered DNA. Biophys. J. 83:3202-3210.
15.	Jin, Q., A. M. Fleming, C. J. Burrows, and H. S. White. 2012. Unzipping kinetics of duplex DNA containing oxidized lesions in an -hemolysin nanopore. J. Am. Chem. Soc. 134:11006-11011.
16.	Liu, A., Q. Zhao, D. M. M. Krishantha, and X. Guan. 2011. Unzipping of double-stranded DNA in engineered -hemolysin pores. J. Phys. Chem. Lett. 2:1372-1376.
17.	Mathé, J., H. Visram, V. Viasnoff, Y. Rabin, and A. Meller. 2004. Nanopore unzipping of individual DNA hairpin molecules. Biophys. J. 87:3205-3212.

18. Muzard, J., M. Martinho, J. Mathé, U. Bockelmann, and V. Viasnoff. DNA translocation and unzipping through a nanopore: some geometrical effects. Biophys. J. 98:2170-2178.

19. Sauer-Budge, A. F., J. A. Nyamwanda, D. K. Lubensky, and D. Branton. 2003. Unzipping kinetics of double-stranded DNA in a nanopore. Phys. Rev. Lett. 90:238101.

20. Schibel, A. E. P., A. M. Fleming, Q. Jin, N. An, J. Liu, C. P. Blakemore, H. S. White, and C. J. Burrows. 2011. Sequence-specific single-molecule analysis of 8-Oxo-7,8-dihydroguanine lesions in DNA based on unzipping kinetics of complementary probes in ion channel recordings. J. Am. Chem. Soc. 133:14778-14784.

21. Jin, Q., A. M. Fleming, R. P. Johnson, Y. Ding, C. J. Burrows, and H. S. White. 2013. Base-excision repair activity of uracil-DNA glycosylase monitored using the latch zone of -hemolysin. J. Am. Chem. Soc. 135:19347-19353.

22. Pfeifer, G., and A. Besaratinia. 2009. Mutational spectra of human cancer. Hum. Genet. 125:493-506.

23. Bonthuis, D. J., J. Zhang, B. Hornblower, J. Mathé, B. I. Shklovskii, and A. Meller. 2006. Self-energy-limited ion transport in subnanometer channels. Phys. Rev. Lett. 97:128104.

24. Drew, H. R., R. M. Wing, T. Takano, C. Broka, S. Tanaka, K. Itakura, and R. E. Dickerson. 1981. Structure of a B-DNA dodecamer: conformation and dynamics. Proc. Natl. Acad. Sci. USA 78:2179-2183.

25. Kang, X. F., L.-Q. Gu, S. Cheley, and H. Bayley. 2005. Single protein pores containing molecular adapters at high temperatures. Angew. Chemie Int. Ed. 44:1495-1499.

26. Longsworth, L. G. 1954. Temperature dependence of diffusion in aqueous solutions. J. Phys. Chem. 58:770-773.

27. Owczarzy, R., Y. You, B. G. Moreira, J. A. Manthey, L. Huang, M. A. Behlke, and J. A. Walder. 2004. Effects of sodium ions on DNA duplex oligomers: improved predictions of melting temperatures. Biochem. 43:3537-3554.

28. Altan-Bonnet, G., A. Libchaber, and O. Krichevsky. 2003. Bubble dynamics in double-stranded DNA. Phys. Rev. Lett. 90:138101.

29. Fei, J., and T. Ha. 2013. Watching DNA breath one molecule at a time. Proc. Natl. Acad. Sci. USA 110:17173-17174.

30. Phelps, C., W. Lee, D. Jose, P. H. von Hippel, and A. H. Marcus. 2013. Single-molecule FRET and linear dichroism studies of DNA breathing and helicase binding at replication fork junctions. Proc. Natl. Acad. Sci. USA 110:17320-17325.

31. Nielsen, P. E., M. Egholm, and O. Buchardt. 1994. Peptide nucleic acid (PNA). A DNA mimic with a peptide backbone. Bioconj. Chem. 5:3-7.

32. White, R. J., E. N. Ervin, T. Yang, X. Chen, S. Daniel, P. S. Cremer, and H. S. White. 2007. Single ion-channel recordings using glass nanopore membranes. J. Am. Chem. Soc. 129:11766-11775.